

## Radicals

## Rational Design of a Phosphorus-Centered Disbiradical

Jan Rosenboom, Florian Taube, Leon Teichmeier, Alexander Villinger, Maik Reinhard, Serhiy Demeshko, Marina Bennati, Jonas Bresien,\* Björn Corzilius,\* and Axel Schulz\*

In memory of Edgar Niecke (1939–2023)

**Abstract:** Phosphorus-centered disbiradicals, in which the radical sites exist as individual spin doublets with weak spin-spin interaction have not been known so far. Starting from monoradicals of the type  $[\text{P}(\mu\text{-N}^{\bullet}\text{Ter})_2\text{P-R}]$ , we have now succeeded in linking two such monoradical phosphorus centers by appropriate choice of a linker. To this end, biradical  $[\text{P}(\mu\text{-N}^{\bullet}\text{Ter})_2\text{P}^*]$  (**1**) was treated with 1,6-dibromohexane, affording the brominated species  $\{\text{Br}[\text{P}(\mu\text{-N}^{\bullet}\text{Ter})_2]_2\text{C}_6\text{H}_{12}$  (**3**). Subsequent reduction with  $\text{KC}_8$  led to the formation of the disbiradical  $[\text{P}(\mu\text{-N}^{\bullet}\text{Ter})_2]_2\text{C}_6\text{H}_{12}$  (**4**) featuring a large distance between the radical phosphorus sites in the solid state and formally the highest biradical character observed in a P-centered biradical so far, approaching 100%. EPR spectroscopy revealed a three-line signal in solution with a considerably larger exchange interaction than would be expected from the molecular structure of the single crystal. Quantum chemical calculations revealed a highly dynamic conformational space; thus, the two radical sites can approach each other with a much smaller distance in solution. Further reduction of **4** resulted in the formation of a potassium salt featuring the first structurally characterized P-centered distonic radical anion (**5**). Moreover, **4** could be used in small molecule activation.

**B**iradicals are molecular entities with two unpaired electrons that can be classified by the interaction between the two electron spins (Figures 1 and 2),<sup>[1–3]</sup> which can be described by the electron exchange coupling constant  $J$

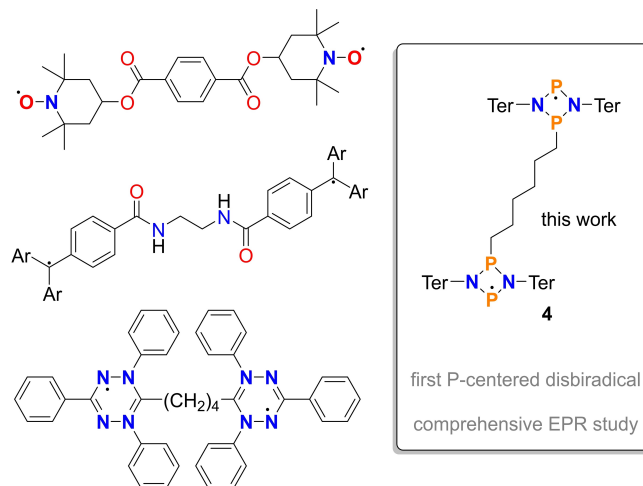


**Figure 1.** Left: Selected examples of O-, N-, and C-centered disbiradicals. Top: nitroxide<sup>[2]</sup>, middle: trityl<sup>[4]</sup>, and bottom: verdazyl<sup>[5]</sup>-based disbiradicals. Right: Bis-cyclo-diphospho-diazene-diyl (**4**) featuring two phosphorus radical sites.

(note that throughout the paper the convention  $\hat{H} = -2J\hat{S}_1\hat{S}_2$  will be used for the description of the isotropic exchange interaction). In case of  $J \approx 0$ , the interaction is negligible, the biradical is a two-doublet species, and has recently been termed a disbiradical.<sup>1</sup> Selected examples are shown in Figure 1. If  $J \neq 0$  the species can be called a biradical(oid) and is either a singlet species ( $J < 0$ , antiferromagnetic coupling) or a triplet species ( $J > 0$ , ferromagnetic coupling, Figure 2). These different types of biradicals feature a different behavior in EPR experiments. While

[\*] J. Rosenboom, F. Taube, L. Teichmeier, Dr. A. Villinger, Dr. J. Bresien, Prof. Dr. B. Corzilius, Prof. Dr. A. Schulz  
 Institut für Chemie, Universität Rostock  
 Albert-Einstein-Straße 3a, 18059 Rostock (Germany)  
 E-mail: jonas.bresien@uni-rostock.de  
 bjoern.corzilius@uni-rostock.de  
 axel.schulz@uni-rostock.de  
 Homepage: <http://www.schulz.chemie.uni-rostock.de/>  
 Prof. Dr. B. Corzilius, Prof. Dr. A. Schulz  
 Leibniz-Institut für Katalyse e.V.  
 Albert-Einstein-Straße 29a, 18059 Rostock (Germany)  
 M. Reinhard, Dr. S. Demeshko, Prof. Dr. M. Bennati  
 Georg-August-Universität Göttingen  
 Tammannstr. 4/6, 37077 Göttingen (Germany)

Prof. Dr. B. Corzilius  
 Department Life, Light & Matter, Universität Rostock  
 Albert-Einstein-Straße 25, 18059 Rostock (Germany)

M. Reinhard, Prof. Dr. M. Bennati  
 MPINAT, Research Group ESR Spectroscopy, Max Planck Institute  
 for Multidisciplinary Sciences  
 Am Fassberg 11, 37077 Göttingen (Germany)

© 2023 The Authors. Angewandte Chemie International Edition published by Wiley-VCH GmbH. This is an open access article under the terms of the Creative Commons Attribution License, which permits use, distribution and reproduction in any medium, provided the original work is properly cited.

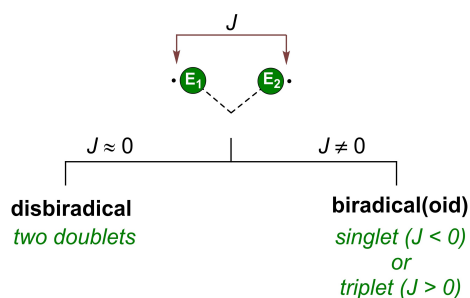


**Figure 2.** Classification of biradicals (E = any arbitrary atom containing an unpaired electron).

open-shell singlet biradicals like [ $\text{P}(\mu\text{-N}^{\text{Ter}})_2\text{P}^*$ ] (**1**, Ter = 2,6-dimesitylphenyl) are EPR silent as their spin density is zero, triplet biradicals and disbiradicals show distinct EPR spectra. The form of an EPR signal associated with a disbiradical depends on the ratio between the electron-electron exchange interaction  $J$  and the hyperfine coupling  $A$  as illustrated in Figure 3.

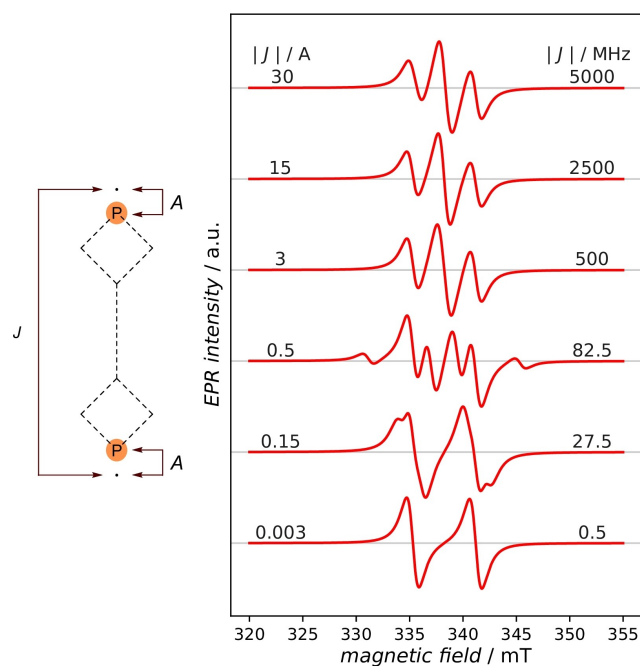
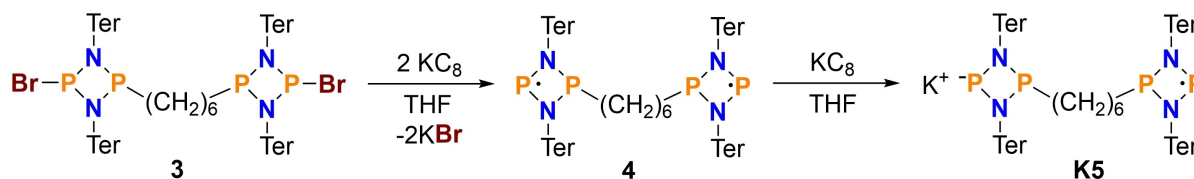


**Figure 3.** Comparison of simulated EPR signals arising from a symmetric P-centered disbiradical depending on the  $|J|/A$  ratio ( $g_{\text{iso}} = 2.0023$ ,  $A_{\text{iso}}(^{31}\text{P}) = 165$  MHz,  $S = 1/2$ ,  $lw = 2$  mT (100% LORENTZIAN, FWHM),  $\omega_{\mu\text{w}} = 9.48$  GHz).

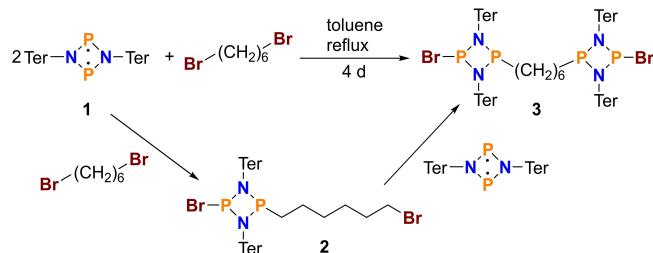


**Scheme 2.** Reduction of **3** with  $\text{KC}_8$  yields disbiradical **4**. Overreduction leads to the formation of the potassium salt **K5** exhibiting a distonic radical anion  $5^-$ .

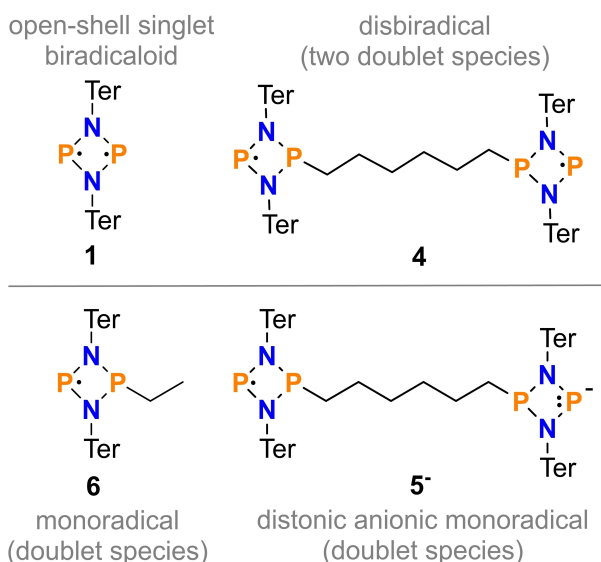
Figure 3 showcases the EPR signal form depending on various  $J/A$  ratios for a  $^{31}\text{P}$ -centered biradical, with  $J$  varied and  $A$  held constant at 165 MHz. In the limiting case of a large  $J/A$  ratio, a three-line signal is visible. In case of a very small  $J/A$  ratio a two-line signal expected from a P-centered monoradical can be observed. Note that from a ratio  $|J|/A > \approx 3$  no clear statement can be made about the strength of the  $J$  coupling. In this case ( $|J| \gg A$ ), such a system can better be described by an effective spin  $S = 1$ , coupling with  $A/2$  to two, in this specific case, equivalent nuclei without specification of the value of the  $J$ -coupling. This phenomenon was first described in copper acetate and also in other systems such as TSCHITSCHIBABIN type biradicals.<sup>[6,7]</sup>

Various classes of biradicals have been built up by combining two persistent monoradical units (nitroxides, verdazyls, triphenylmethyl (trityl) etc., Figure 1) with diverse conjugated and non-conjugated organic bridges.<sup>[1,8]</sup> The structural and electronic nature of the bridge results in a varying degree of interaction between the two unpaired electrons relevant for the usage as polarizing agents in DNP (Dynamic Nuclear Polarization) NMR spectroscopy.<sup>[4,9–11]</sup> Here we want to report on a novel phosphorus-centered disbiradical and its electronic and chemical properties.

Monoradicals of the type [ $\text{P}(\mu\text{-N}^{\text{Ter}})_2\text{P-R}$ ] can be prepared by addition of a bromoalkane,  $\text{R-Br}$ , to the well-known biradical [ $\text{P}(\mu\text{-N}^{\text{Ter}})_2\text{P}^*$ ] (**1**) and subsequent reduction.<sup>[12]</sup> We now ask whether an analogous reaction with a dibromo-alkane would then lead to the desired disbiradical **4** (Schemes 1–3). For a sufficiently large distance between the radical centers to minimize their interaction, the alkane chain had to consist of at least a hexyl unit. Utilizing this bromoalkane route, it was indeed possible to add 1,6-dibromohexane to [ $\text{P}(\mu\text{-N}^{\text{Ter}})_2\text{P}^*$ ] (**1**) in a 1:1 stoichiometry forming dibromo-precursor **2** in 52% isolated yield (Scheme 1). When **2** was reacted with another equiv-



**Scheme 1.** Reaction between **1** and 1,6-dibromohexane forming **2** and bridged dibromo-precursor **3** depending on the used stoichiometry.



**Scheme 3.** Mono- and biradicals with a *cyclo*-diphospha-diaza-ring.

alent of **1** the desired bridged dibromo-substituted species **3** could be isolated. Compound **3** was also directly accessible on a gram scale when a 2:1 stoichiometry of **1** to 1,6-dibromohexane was applied from the beginning (yield = 68%). Due to the large steric demand of the Ter substituents the reaction required high temperatures and long reaction times (111 °C over 4 d) compared to bromoalkanes with a smaller alkyl chain (minutes to days at RT).<sup>[12]</sup> Products **2** and **3** were fully characterized (see ESI, Figures S3–S6). Reduction of **3** with  $\text{KC}_8$  in THF led to the formation of the desired disbiradical **4** in good yields (59%, Scheme 2), which was immediately indicated by a color change to dark red.

It is important to know that the product distribution (purity) and yields depend strongly on the reaction control, especially on the stoichiometry. For example, when **3** and two equivalents of  $\text{KC}_8$  were combined in the solid and then the solvent was added, over-reduction occurred due to the low solubility of **3** in THF, resulting in the partial formation of potassium salt **K5** bearing the distonic radical anion **5<sup>-</sup>** (Scheme 2). However, when the  $\text{KC}_8$  was added to a suspension of **3** in several small portions over a period of 15 min and the reaction mixture was then filtered over *celite*<sup>®</sup>, pure single-crystalline **4** could be obtained in moderate yields (50–60%, Figures 4 and 5). The oxygen- and moisture-sensitive disbiradical **4** was long term stable when stored in a sealed ampoule under inert gas. Thermally, it decomposed at 200 °C while loss of solvent from the single crystals was already observed at 109 °C (for DSC data see Figure S7). As species **4** is paramagnetic, when crystals were dissolved in  $\text{C}_6\text{D}_6$  and  $^{31}\text{P}$  NMR spectra were recorded, no signals for **4** were detected, while in the  $^1\text{H}$  NMR spectrum only signals of the co-crystallized THF molecules were visible. Dark red crystals of **4** crystallized from THF in the orthorhombic space group *Fddd* with eight formula units and six co-crystallized solvent molecules per cell. There are no close intermolecular contacts between molecules of **4** in

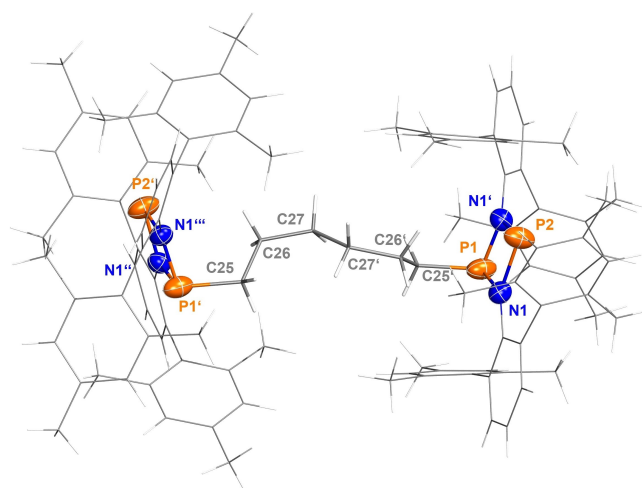


**Figure 4.** Molecular structure of the disbiradical **4** in the crystal. Thermal ellipsoids at 50% probability (123 K). Ter substituents and alkyl bridge depicted as wireframe for clarity. Selected bond lengths (Å) and torsion angles [°]: N1–P1 1.749(4), N1'–P1 1.673(4), N1–P2 1.805(4), N1'–P2 1.683(4), P1–C25' 1.85(1), P2...P2' 10.913(6); P1–N1–N1'–P2 178.0(2), N1–P1–N1'–C25 101.2(4), N1'–P1–N1–C25 102.4(4).

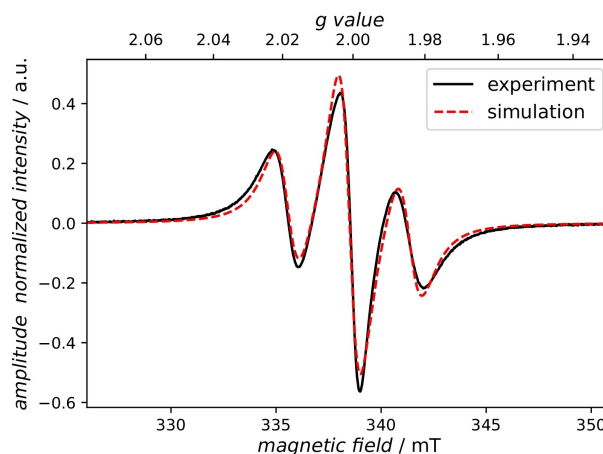


**Figure 5.** X-band (9.48 GHz) EPR spectrum of **4** in THF,  $T = 293$  K ( $S = 1$ ,  $g_{\text{iso}} = 2.001$ ,  $A_1(^{31}\text{P})/2 = A_2(^{31}\text{P})/2 = -40$  MHz,  $A_3(^{31}\text{P})/2 = 324$  MHz,  $l\omega = 1.713$  mT (100% LORENTZIAN, FWHM),  $\tau_R = 0.035$  ns) (for details on simulation see below).

the crystal. The molecular structure is determined by its  $C_2$  symmetry with an intersection of three  $C_2$ -axes resulting in a disorder over two molecule layers (overall  $D_2$  symmetry, cf. Figure S1). Both radical phosphorus centers (P2/P2'), separated by 10.913(5) Å, sit in pockets that are well protected by the four bulky Ter substituents, as depicted in Figure 4. The most prominent structural feature of **4** is the two nearly planar  $\text{P}_2\text{N}_2$  four-membered heterocycles bridged by a hexyl group (deviation from planarity  $< 2^\circ$ ). All four P–N distances are different (1.673(4)–1.805(4) Å) and are in the range of polar P–N single bonds (cf.  $\Sigma r_{\text{cov}}(\text{P–N}) = 1.82$  Å).<sup>[13]</sup>

As expected, computations of **4** confirm that it is a phosphorus-centered disbiradical (a two-doublet species).

The MULLIKEN spin density is mainly localized at the divalent P2 ( $\approx 0.75$ , cf.  $0.70$  [ $\bullet\text{P}(\mu\text{-N-Ter})_2\text{P-Et}$ ] (**6**), Scheme 3);<sup>[12]</sup> while only small values are computed for N1 (0.03) and N1' (0.03), respectively (Figure S23). The large distance of  $10.913(6)$  Å (calcd.  $10.39$  Å) between the two P atoms containing the unpaired electrons does not allow for any significant dipole-dipole interaction in the solid state (Figure 4 and Figure 6), and, additionally, the unconjugated hexyl linker leads to vanishing electron-electron exchange interaction by conjugation. It was all the more surprising that solution EPR experiments (Figure 5) with pure **4** yielded a spectrum with a 1:2:1 triplet (See Supporting Information section 5.1.4), typical of a biradical with a sizeable interaction between the two electrons. The line shape of the experimental spectra clearly indicates a  $J$ -coupling of  $>1$  GHz when compared to simulations (Figure 3) and thus comes to the limit of what can be sensibly detected in X-band. From this observation, it was clear that the structure in solution must be subject to dynamics that cause the two radical P-atoms to approach each other.

Therefore, a conformer search using CREST<sup>[14,15]</sup> and CENSO<sup>[16]</sup> together with GFN-FF force field<sup>[17]</sup> and GFN2-xTB<sup>[18]</sup>//GFN-FF composite methods was performed. The screening of more than 60000 structures (500 conformers) revealed that in solution the most favorable structures are the ones with a much shorter P2...P2' distance. The most energetically favorable and therefore dominant conformer in solution (T1,  $x = 47\%$ , Figure 6; cf. Figure S21 for more details and other conformers) has a P2...P2' distance of only  $7.31$  Å and is energetically stabilized with respect to the conformer observed in the solid state (T5,  $d(\text{P2}\cdots\text{P2}') = 10.39$  Å) by  $17$  kJ/mol. Hence, the peculiar EPR signal of **4** in solution can be explained by exchange coupling of the two electrons not through the unconjugated  $\text{CH}_2$ -chain but “through space” in accord with computed EPR data (Table S6).

The EPR signal of **4** in solution was investigated at different temperatures (Figure 7) and with different microwave frequencies (X-band/Q-band). At higher temperatures, an increase in the amplitude of the outer transitions occurred which allows an investigation of dynamic effects within the system caused by partial averaging of the  $g$ - and  $A$ -anisotropies by rotational diffusion of the molecule.<sup>[19,20]</sup> A deviation of the spin system from the isotropic limit seems conceivable considering the high molar mass of  $M = 1517$  g/mol. To get access to the  $g$ - and  $A$ -tensors a spectrum of the Et-substituted monoradical **6** was recorded in frozen solution (See Supporting Information section 5.1.2) and evaluated. With this data, simulations were performed taking into account the isotropic rotation-correlation time  $\tau_R$  which varies between  $0.005$  ns and  $0.152$  ns depending on the measurement temperature. These correlation times are at least an order of magnitude shorter than what is expected from the STOKES-EINSTEIN-DEBYE equation for a rigid spherical particle. Therefore, we conclude that internal conformational dynamics are allowing the radical moieties to reorient on a much faster timescale than the molecule as whole. The fact that all spectra can easily be reproduced considering a  $S = 1$  system coupling to

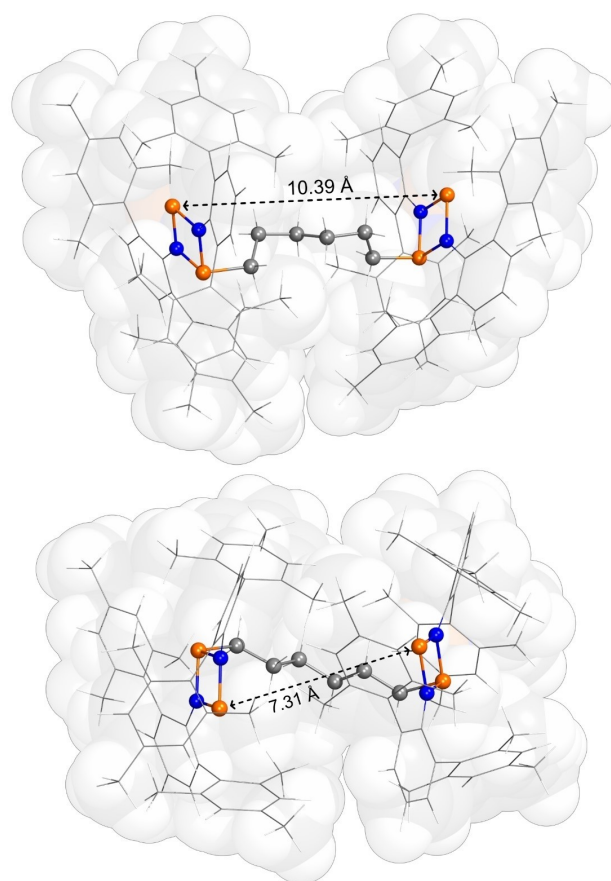


**Figure 6.** Comparison of the optimized molecular structures originating from the solid state data (T5, top) and most favorable conformer in toluene solution (T1, bottom; conformer search using CREST/CENSO, GFN2-xTB<sup>[18]</sup>//GFN-FF, optimization at B97-3c, solvent correction for toluene)

two equivalent phosphorous atoms with  $A(^{31}\text{P})/2$  demonstrates that the resulting dynamically averaged  $J$  must still be much larger than the isotropic  $A(^{31}\text{P})$  and that isotropic (exchange)  $J$  is dominating over dipolar e-e interaction.

An EPR spectrum of a single crystal of **4** in the solid state was also measured. However, the intramolecular electron-electron interaction was not visible due to the high spin concentration causing a loss of all information about the (hyper-)fine structure and only one broad transition was observed (Figure S16). A Q-band EPR spectrum of **4** in solution could be simulated<sup>[21-23]</sup> using the parameters from the X-band series of Figure 7 (see Supporting Information section 5.1.5 for Q-band EPR spectrum and simulation), showing the consistency of our set of anisotropy parameters and correlation time at different field strengths.

In light of the definition of the term disbiradical ( $J \approx 0$ , vide infra), one could assume that a disbiradical is indeed present in the single crystal of species **4**, considering the expectedly small electron-electron interaction and the relatively larger  $A$ -anisotropy. In contrast, in solution a dynamic conformational change occurs which gives rise to clear experimental evidence of an EPR spectroscopically significant electron-electron coupling dominating over the iso-

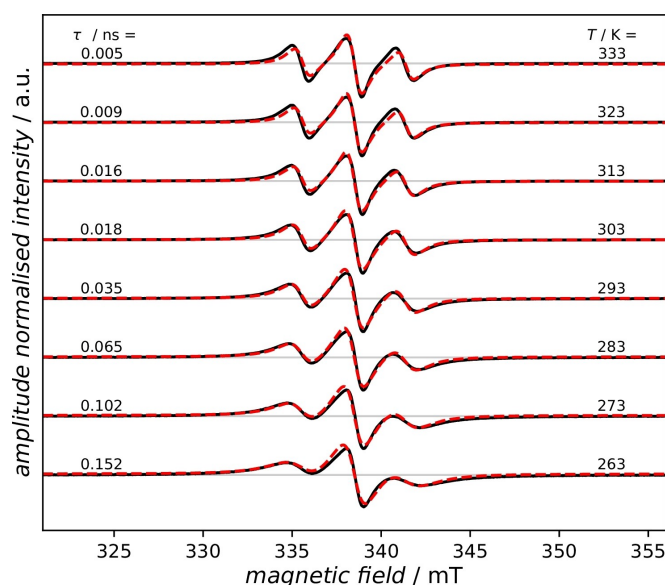


**Figure 7.** X-band (9.48 GHz) EPR spectra of **4** dissolved in THF at different temperatures. The hyperfine interaction tensor **A** determined from simulation of the experimental EPR spectrum of **6** at 100 K was kept constant for the different temperatures, varying only the rotational correlation time  $\tau_R$  (See Supporting Information section 5.1.3 for further information and simulation parameters).

tropic EPR parameters. But the question now arises whether such a species can generally still be considered a diradical. This ultimately leads us to the dilemma to define at what magnitude of interaction the transition from a diradical to a biradical(oid) occurs, and it is worth noting that this transition is continuous, and also depends on the external conditions of the experiment (i.e., can the two doublet centers be spectroscopically distinguished with respect to their interaction). Equally interesting is the differing perspective from molecular chemists and spectroscopists about what is considered to be a significant interaction between the two unpaired electrons in a biradical. For example, the coupling constant  $J$  of  $> 500$  MHz as observed in the solution EPR spectrum equals a singlet-triplet energy gap ( $\Delta E_{S-T}$ ) of  $> 4.0 \times 10^{-4}$  kJ/mol which from a chemical reactivity point of view indicates virtually degenerate singlet and triplet states. Therefore, we refer to **4** as a diradical despite the observed three-line signal in the solution EPR spectrum.

The singlet-triplet energy gap was additionally estimated using magnetic susceptibility measurements on a SQUID magnetometer. Experimental data were modelled with the *julX* program<sup>[24]</sup> using a fitting procedure to the spin Hamiltonian  $\hat{H} = -2J\hat{S}_1\hat{S}_2 + g\mu_B\mathbf{B}(\hat{S}_1 + \hat{S}_2)$ . The coupling constant  $J$  amounted to  $-0.19$  cm<sup>-1</sup> equaling to a  $\Delta E_{S-T}$  of  $-0.38$  cm<sup>-1</sup> or about  $-4.5 \times 10^{-3}$  kJ/mol indicating a singlet ground state with a biradical character of virtually 100% (see Figure S24). As intermolecular interactions also play a role in the solid compared to a low-concentrated sample in solution, this is to be considered as a maximum value and is thus in good agreement with the data obtained by EPR

spectroscopy and computations ( $\Delta E_{S-T} = -3.2 \times 10^{-3}$  kJ/mol, see Supporting Information section 6.2 for details).

After the synthesis of pure **4**, we also tried to reduce it further selectively to obtain the pure distonic radical anion **5<sup>-</sup>** as potassium salt **K5** (Scheme 2). However, this proved to be very difficult. Even with long reaction times and a large excess of  $KC_8$ , it was impossible to obtain pure **K5**. Reaction EPR spectra and NMR data suggest overreduction of **5** towards a Ter-phosphide<sup>[25]</sup> while **4** was still detectable (Figure S12). Hence, only mixed single crystals of **4** and **K5** with varying ratios of both compounds could be isolated. As determined by single crystal XRD they crystallized very similarly to pure **4** in the orthorhombic space group *Fddd*. (See ESI for details). The molecular structure of **K5** is displayed in Figure 8. The mixed single crystals were also dissolved and an X-band EPR spectrum of the resulting mixture of **4** and **K5** (83% to 17%) was measured (Figure 9).

Due to the structural similarities, the *g*-factors and coupling constants *A* of the two compounds are virtually identical and therefore the two signals are superimposed. As in **5<sup>-</sup>** only one unpaired electron is present (doublet species), this results in a two-line signal due to the coupling with one <sup>31</sup>P nucleus. As depicted in Scheme 3, the radical moiety of **5<sup>-</sup>** is also structurally and electronically similar to the ethyl substituted monoradical **6** previously synthesized by our group.<sup>[12]</sup>

Therefore, it was possible to simulate<sup>[21–23]</sup> the EPR spectrum of a solution of **4/K5** mixed crystals by using the EPR parameters from pure **4** and the pure ethyl substituted monoradical **6**, magnetically virtually equivalent to **5<sup>-</sup>**, and applying the ratios derived from single crystal XRD of the same sample. By this procedure, it was possible to obtain

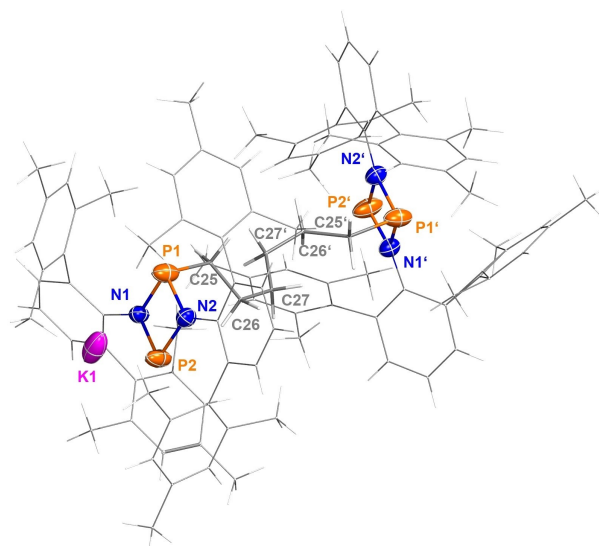


**Figure 8.** Molecular structures of the salt **K5** bearing the distonic radical anion **5<sup>-</sup>** in the crystal. Thermal ellipsoids at 50% probability (123 K). Ter substituents depicted as wireframe for clarity. Selected bond lengths (Å) and torsion angles [°]: N1–P1 1.70(1), N2–P1 1.771(9), N2–P2 1.74(1), N1–P2 1.71(1), P1–C25 1.879(7), K1–P2 2.810(7), P1–N1–N2–P2 179.1(7), N1–P1–N2–C25 97.6(5).

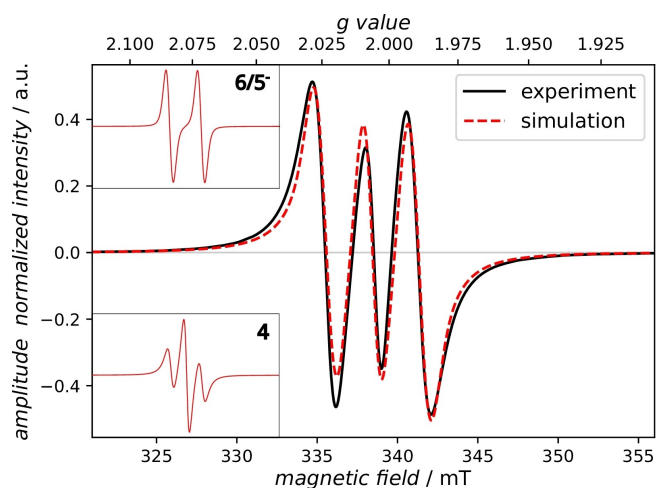


**Figure 9.** X-band (9.48 GHz) EPR spectrum and simulation of a mixture (83:17) of **4** and **K5** in toluene; simulated spectra of pure components are shown in inserts (magnetic field axis at same scale). EPR parameters for pure components in toluene: Monoradical:  $S = 1/2$ ,  $g_{\text{iso}} = 2.0011$ ,  $A_{\text{iso}}(^{31}\text{P}) = 164$  MHz,  $l\omega = 1.1$  mT : 1 mT (GAUSSIAN : LORENTZIAN, FWHM); Biradical:  $S = 1$ ,  $g_{\text{iso}} = 2.001$ ,  $A_1(^{31}\text{P})/2 = A_2(^{31}\text{P})/2 = -40$  MHz,  $A_3(^{31}\text{P})/2 = 324$  MHz,  $l\omega = 1.713$  mT (100% LORENTZIAN, FWHM),  $\tau_{\text{R}} = 0.044$  ns. Simulation was done by using ratios obtained from single crystal XRD and EPR parameters of pure **4** and pure ethyl substituted monoradical **6**. See Supporting Information section 5.1.6. for details.

the simulated spectrum in Figure 9 despite the lack of a pure sample of **K5**, proving that EPR and XRD data are coherent. Although numerous P-centered monoradicals are known,<sup>[26–28]</sup> to the best of our knowledge there are no examples of structurally characterized P-centered distonic radical anions.<sup>[29–31]</sup>

Finally, first preliminary reactivity studies with **4** showed that it does not react with  $\text{H}_2$  (1 atm, 60 °C, 3 h). However, when exposed to acetylene several new species were detected by  $^{31}\text{P}$  NMR spectroscopy indicating poly-/oligomerization (Figure S18).

In summary, the synthesis of a phosphorus-based disbiradical **4** was achieved by introducing an innocent hexyl ligand (Scheme 3). **4** isomerizes in solution, forming conformers with significant shorter distances between the radical sites which can thereby interact weakly by partial overlap of the spin-carrying orbitals through space. Starting from brominated precursor **3**, a salt with a distonic monoradical anion was also synthesized by further reduction. In preliminary studies, **4** was used in small molecule activation chemistry and is to be applied as polarization transfer reagents in DNP NMR spectroscopy.

### Supporting Information

The authors have cited additional references within the Supporting Information.<sup>[32–73]</sup> Deposition numbers 2304337 (for **2**), 2304336 (for **3**), 2304333 (for **4**), 2304334 (for **4/K5**), 2304335 (for **7**) contain the supplementary crystallographic data for this paper. These data are provided free of charge

by the joint Cambridge Crystallographic Data Centre and Fachinformationszentrum Karlsruhe Access Structures service.

### Acknowledgements

J.R. wants to thank the Konrad-Adenauer-Stiftung for financial and non-material support. Additionally, we thank Dr. Edgar Zander for help in the lab. We wish to thank the ITMZ at the University of Rostock for access to the cluster computer. This project received funding from the Deutsche Forschungsgemeinschaft (DFG; SCHU 1170/12-2, SFB TRR 386 TRR 386-A2). Purchase of the SQUID magnetometer was enabled by the Deutsche Forschungsgemeinschaft (DFG, German Research Foundation, project number INST 186/1329-1 FUGG) and the Niedersächsische Ministerium für Wissenschaft und Kultur (MWK); purchase of the EPR spectrometer was supported by the European Union through EFRE grant GHS-21-0005. Open Access funding enabled and organized by Projekt DEAL.

### Conflict of Interest

The authors declare no conflict of interest.

### Data Availability Statement

The data that support the findings of this study are available in the supplementary material of this article.

**Keywords:** Biradical · Diradical · Distonic Radical Anion · EPR Spectroscopy · Phosphorus Chemistry

- [1] A. Hinz, J. Bresien, F. Breher, A. Schulz, *Chem. Rev.* **2023**, *123*, 10468–10526.
- [2] M. Abe, *Chem. Rev.* **2013**, *113*, 7011–7088.
- [3] J. Bresien, L. Eickhoff, A. Schulz, E. Zander, in *Comprehensive Inorganic Chemistry III* (Eds.: J. Reedijk, K. R. Poeppelmeier), Elsevier, Oxford, **2023**, pp. 165–233.
- [4] S. Macholl, H. Jóhannesson, J. H. Ardenkjaer-Larsen, *Phys. Chem. Chem. Phys.* **2010**, *12*, 5804–5817.
- [5] B. D. Koivisto, R. G. Hicks, *Coord. Chem. Rev.* **2005**, *249*, 2612–2630.
- [6] B. Bleaney, K. D. Bowers, *Proc. R. Soc. London Ser. A* **1952**, *214*, 451–465.
- [7] P. Ravat, M. Baumgarten, *Phys. Chem. Chem. Phys.* **2015**, *17*, 983–991.
- [8] I. Ratera, J. Veciana, *Chem. Soc. Rev.* **2012**, *41*, 303–349.
- [9] J. Soetbeer, P. Gast, J. J. Walsh, Y. Zhao, C. George, C. Yang, T. M. Swager, R. G. Griffin, G. Mathies, *Phys. Chem. Chem. Phys.* **2018**, *20*, 25506–25517.
- [10] R. Harrabi, T. Halbritter, F. Aussenac, O. Dakhlaoui, J. van Tol, K. K. Damodaran, D. Lee, S. Paul, S. Hediger, F. Mentink-Vigier, S. T. Sigurdsson, G. De Paëpe, *Angew. Chem. Int. Ed.* **2022**, *61*, e202114103.
- [11] G. Menzildjian, J. Schlagnitweit, G. Casano, O. Ouari, D. Gajan, A. Lesage, *Chem. Sci.* **2023**, *14*, 6120–6148.

- [12] J. Rosenboom, L. Chojetzki, T. Suhrbier, J. Rabeah, A. Villinger, R. Wustrack, J. Bresien, A. Schulz, *Chem. Eur. J.* **2022**, *28*, e202200624.
- [13] P. Pyykkö, M. Atsumi, *Chem. Eur. J.* **2009**, *15*, 186–197.
- [14] S. Grimme, *J. Chem. Theory Comput.* **2019**, *15*, 2847–2862.
- [15] P. Pracht, F. Bohle, S. Grimme, *Phys. Chem. Chem. Phys.* **2020**, *22*, 7169–7192.
- [16] S. Grimme, F. Bohle, A. Hansen, P. Pracht, S. Spicher, M. Stahn, *J. Phys. Chem. A* **2021**, *125*, 4039–4054.
- [17] S. Spicher, S. Grimme, *Angew. Chem. Int. Ed.* **2020**, *59*, 15665–15673.
- [18] C. Bannwarth, S. Ehlert, S. Grimme, *J. Chem. Theory Comput.* **2019**, *15*, 1652–1671.
- [19] E. G. Bagryanskaya, D. N. Polovyanenko, M. V. Fedin, L. Kulik, A. Schnegg, A. Savitsky, K. Möbius, A. W. Coleman, G. S. Ananchenko, J. A. Ripmeester, *Phys. Chem. Chem. Phys.* **2009**, *11*, 6700–6707.
- [20] S. Stoll, D. Goldfarb, *EPR Spectroscopy: Fundamentals and Methods*, Wiley, Hoboken, **2018**.
- [21] M. Schröder, T. Biskup, **2023**, <https://doi.org/10.5281/ZENODO.8150469>.
- [22] M. Schröder, T. Biskup, *J. Magn. Reson.* **2022**, *335*, 107140.
- [23] S. Stoll, A. Schweiger, *J. Magn. Reson.* **2006**, *178*, 42–55.
- [24] E. Bill, *JulX, Program for Simulation of Molecular Magnetic Data*, Max-Planck Institute for Chemical Energy Conversion, Mülheim/Ruhr, **2008**.
- [25] A. Hinz, A. Schulz, A. Villinger, *Angew. Chem. Int. Ed.* **2015**, *54*, 668–672.
- [26] B. Das, A. Makol, S. Kundu, *Dalton Trans.* **2022**, *51*, 12404–12426.
- [27] Y. Su, X. Zheng, X. Wang, X. Zhang, Y. Sui, X. Wang, *J. Am. Chem. Soc.* **2014**, *136*, 6251–6254.
- [28] P. P. Power, *Chem. Rev.* **2003**, *103*, 789–810.
- [29] B. F. Yates, W. J. Bouma, L. Radom, *J. Am. Chem. Soc.* **1984**, *106*, 5805–5808.
- [30] K. M. Stirk, L. K. M. Kiminkinen, H. I. Kenttamaa, *Chem. Rev.* **1992**, *92*, 1649–1665.
- [31] D. M. Tomazela, A. A. Sabino, R. Sparrapan, F. C. Gozzo, M. N. Eberlin, *J. Am. Soc. Mass Spectrom.* **2006**, *17*, 1014–1022.
- [32] C. H. Butzlaff, A. X. Trautwein, E. Winkler, *Metallobiochemistry, Pt. D: Physical and Spectroscopic Methods for Probing Metal Ion Environments in Metalloproteins*, Academic Press, New York, **1993**, pp. 412–437.
- [33] E. Bill, *mpView.1.4.1, Program for Viewing and Data Import for Files from MPMS3 SQUID Magnetometer*, Max-Planck Institute for Chemical Energy Conversion, Mülheim/Ruhr, **2021**.
- [34] F. Neese, F. Wennmohs, U. Becker, C. Riplinger, *J. Chem. Phys.* **2020**, *152*, 224108.
- [35] F. Neese, *Wiley Interdiscip. Rev.: Comput. Mol. Sci.* **2022**, *12*, e1606.
- [36] C. Bannwarth, E. Caldeweyher, S. Ehlert, A. Hansen, P. Pracht, J. Seibert, S. Spicher, S. Grimme, *Wiley Interdiscip. Rev.: Comput. Mol. Sci.* **2021**, *11*, e01493.
- [37] J. G. Brandenburg, C. Bannwarth, A. Hansen, S. Grimme, *J. Chem. Phys.* **2018**, *148*, 064104.
- [38] S. Grimme, J. Antony, S. Ehrlich, H. Krieg, *J. Chem. Phys.* **2010**, *132*, 154104.
- [39] S. Grimme, S. Ehrlich, L. Goerigk, *J. Comput. Chem.* **2011**, *32*, 1456–1465.
- [40] F. Weigend, R. Ahlrichs, *Phys. Chem. Chem. Phys.* **2005**, *7*, 3297.
- [41] A. Hellweg, C. Hättig, S. Höfener, W. Klopper, *Theor. Chem. Acc.* **2007**, *117*, 587–597.
- [42] W. Haberditzl, *Angew. Chem. Int. Ed.* **1966**, *5*, 288–298.
- [43] G. A. Bain, J. F. Berry, *J. Chem. Educ.* **2008**, *85*, 532.
- [44] G. M. G. M. Sheldrick, *SADABS*, University Of Göttingen, Germany, University of Göttingen, Germany, **2004**.
- [45] T. Biskup, **2023**, <https://doi.org/10.5281/zenodo.4717937>.
- [46] Origin(Pro), Version 2023. OriginLab Corporation, Northampton, MA, USA.
- [47] G. M. Sheldrick, *Acta Crystallogr. Sect. A* **2015**, *71*, 3–8.
- [48] J. Popp, T. Biskup, *Chem. Methods* **2022**, *2*, e202100097.
- [49] F. Neese, *Wiley Interdiscip. Rev.: Comput. Mol. Sci.* **2012**, *2*, 73–78.
- [50] S. Ehlert, M. Stahn, S. Spicher, S. Grimme, *J. Chem. Theory Comput.* **2021**, *17*, 4250–4261.
- [51] S. Grimme, *J. Comput. Chem.* **2006**, *27*, 1787–1799.
- [52] A. V. Marenich, C. J. Cramer, D. G. Truhlar, *J. Phys. Chem. B* **2009**, *113*, 6378–6396.
- [53] F. Neese, *J. Chem. Phys.* **2001**, *115*, 11080–11096.
- [54] F. Neese, *J. Chem. Phys.* **2003**, *118*, 3939–3948.
- [55] F. Neese, *J. Chem. Phys.* **2005**, *122*, 34107.
- [56] F. Neese, *eMagRes* **2017**, *6*, 1–22.
- [57] B. A. Heß, C. M. Marian, U. Wahlgren, O. Gropen, *Chem. Phys. Lett.* **1996**, *251*, 365–371.
- [58] J. P. Perdew, K. Burke, M. Ernzerhof, *Phys. Rev. Lett.* **1996**, *77*, 3865–3868.
- [59] J. P. Perdew, K. Burke, M. Ernzerhof, *Phys. Rev. Lett.* **1997**, *78*, 1396–1396.
- [60] C. Adamo, V. Barone, *J. Chem. Phys.* **1999**, *110*, 6158–6170.
- [61] F. Neese, F. Wennmohs, A. Hansen, U. Becker, *Chem. Phys.* **2009**, *356*, 98–109.
- [62] D. Hegarty, M. A. Robb, *Mol. Phys.* **1979**, *38*, 1795–1812.
- [63] R. H. A. Eade, M. A. Robb, *Chem. Phys. Lett.* **1981**, *83*, 362–368.
- [64] H. B. Schlegel, M. A. Robb, *Chem. Phys. Lett.* **1982**, *93*, 43–46.
- [65] F. Bernardi, A. Bottoni, J. J. W. McDouall, M. A. Robb, H. B. Schlegel, *Faraday Symp. Chem. Soc.* **1984**, *19*, 137.
- [66] P. E. M. Siegbahn, *Chem. Phys. Lett.* **1984**, *109*, 417–423.
- [67] M. A. Robb, U. Niazzi, in *Reports in Molecular Theory, Vol. 1* (Eds.: H. Weinstein, G. Náráy-Szabó), CRC Press, Boca Raton, **1990**, pp. 23–55.
- [68] M. J. Frisch, I. N. Ragazos, M. A. Robb, H. B. Schlegel, *Chem. Phys. Lett.* **1992**, *189*, 524–528.
- [69] N. Yamamoto, T. Vreven, M. A. Robb, M. J. Frisch, H. B. Schlegel, *Chem. Phys. Lett.* **1996**, *250*, 373–378.
- [70] M. Klene, M. A. Robb, M. J. Frisch, P. Celani, *J. Chem. Phys.* **2000**, *113*, 5653–5665.
- [71] F. Weigend, *Phys. Chem. Chem. Phys.* **2006**, *8*, 1057.
- [72] T. Soda, Y. Kitagawa, T. Onishi, Y. Takano, Y. Shigeta, H. Nagao, Y. Yoshioka, K. Yamaguchi, *Chem. Phys. Lett.* **2000**, *319*, 223–230.
- [73] J.-P. Malrieu, G. Trinquier, *J. Phys. Chem. A* **2012**, *116*, 8226–8237.

Manuscript received: November 29, 2023

Accepted manuscript online: December 20, 2023

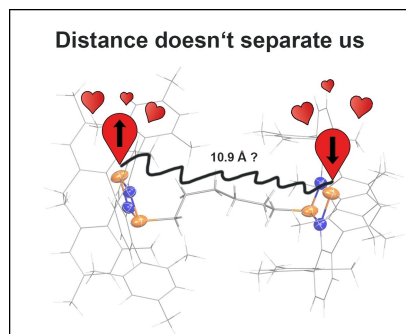
Version of record online: ■■■■■

## Communications

## Radicals

J. Rosenboom, F. Taube, L. Teichmeier,  
A. Villinger, M. Reinhard, S. Demeshko,  
M. Bennati, J. Bresien,\* B. Corzilius,\*  
A. Schulz\* \_\_\_\_\_ e202318210

Rational Design of a Phosphorus-Centered  
Disbiradical



The first synthesis of a phosphorus-centered disbiradical that exhibits highly dynamic behavior in solution leading to isomerization is presented. Among the various conformers, those that have significantly shorter distances between radical sites and thus can interact weakly through space dominate.